SUPPLEMENTARY INFORMATION

Exclusive detection of ethylene using metal oxide chemiresistors with a Pd–V_2O_5–TiO_2 yolk-shell catalytic overlayer *via* heterogeneous Wacker oxidation

Young Kook Moon‡ [a], Ju Hyeong Kim‡ [a], Seong-Yong Jeong[a,b], Soo Min Lee[a], Seon Ju Park[a], Tae Hyun Kim[a], Jong-Heun Lee[a], and Yun Chan Kang* [a]

[a]*Department of Materials Science and Engineering, Korea University, Anam-Dong, Seongbuk-Gu, Seoul 136-713, Republic of Korea, E-mail: yckang@korea.ac.kr; Fax: (+82) 2-928-3584*

[b]*Department of Nanoengineering, University of California, San Diego, 9500 Gilman Drive, La Jolla, CA 92122, USA*

* Corresponding author. E-mail: yckang@korea.ac.kr (Yun Chan Kang)

‡ These authors contributed equally to this work.

Supplementary Materials and Methods

Material characterization

High-resolution scanning electron microscopy (HR-SEM; SU-70, Hitachi Co. Ltd., Japan) was used to observe the morphologies and microstructures of the materials and sensor films. The high-resolution transmission electron microscopy (HR-TEM) and elemental mapping images of the In_2O_3 and Pd–V_2O_5–TiO_2 powders were obtained using Cs-scanning transmission electron microscopy (Cs-STEM, JEM-ARM200F, JEOL Co. Ltd., Japan). The pore size distribution and specific surface area were measured based on the Brunauer–Emmett–Teller (BET) analysis of nitrogen adsorption isotherms (TriStar 3000, Micromeritics, USA). The phase and crystallinity of all the materials were analyzed by X-ray diffraction (XRD) (D/MAX-2500 V/PC, Rigaku, Japan) with a Cu Kα radiation source (λ = 1.5418 Å). The chemical states of Pd and V_2O_5 on TiO_2 were analyzed using X-ray photoelectron spectroscopy (XPS) (X-tool, Ulvac PHI, Japan). The concentrations of Pd and V on the TiO_2 yolk-shell spheres were determined using an inductively coupled plasma-optical emission spectrometer (ICP-OES, iCAP 6300 SERIES, Thermo Fisher Scientific Inc., USA). The cross-sectional images and composition of the 2Pd–V_2O_5–TiO_2/In_2O_3 sensor were investigated using a field-emission electron probe microanalysis (FE-EPMA, JXA-8530F, JEOL Co. Ltd., Japan) apparatus. The reducibility of the 2Pd–V_2O_5–TiO_2 and V_2O_5–TiO_2 catalysts was examined through temperature-programmed reduction by H_2 gas (H_2-TPR) under gradually increasing thermal conditions from room temperature to 500 °C.

Sensor data acquisition

The sensors were heat-treated at 500 °C for 2 h for thermal stabilization before measurement. The sensors were placed in a specially designed quartz tube (inner volume: 1.5 cm^3). The gas concentrations were controlled by mixing the analyte gas and synthetic air using an automatic gas mixing system, and the gas atmosphere was switched using a four-way valve to ensure a constant flow rate (200 cm^3 min^{-1}). The two-probe direct current (DC) resistance was measured

using an electrometer (6487 picoammeter/voltage source, Keithley, USA) interfaced with a computer. The gas responses (R_a/R_g–1, R_a: resistance in air, R_g: resistance in gas) to 1 ppm of ethylene, ethanol, trimethylamine (TMA), carbon monoxide (CO), hydrogen sulfide (H_2S), and hydrogen (H_2) were measured in the temperature range of 300–400 °C.

Catalytic evaluation of Pd–V_2O_5–TiO_2

The catalytic activity of the Pd–V_2O_5–TiO_2 powder was evaluated in a quartz tube reactor (length: 400 mm, inner diameter: 8 mm) kept in a furnace. Afterward, 0.01 g of the 2Pd–V_2O_5–TiO_2 powder was loaded onto a quartz wool bed placed in the middle of the quartz tube. The total flow rate of the 1 ppm ethylene (21% O_2/N_2 balance) was 200 cm^3 min^{-1}. The ethylene conversion and by-product gases in the ethylene oxidation were analyzed by online PTR-QMS (PTR-QMS 300, Ionicon Analytik, Austria). The drift tube conditions were fixed (voltage: 600 V, temperature: 80 °C, pressure: 2.3 mbar), and the electric field strength/gas number density (E/N) was 136 Td (1 Td = 10^{-17} V cm^2). The H_3O^+ ions served as the primary ions, and the catalytic activity tests were carried out at temperatures ranging from 100 to 450 °C.

Detection of ethylene generated from banana

The banana was stored in open air (relative humidity of 50 – 60%) at room temperature (20–25 °C) without any treatment, and the changes in the peel color and the concentration of emitted ethylene were monitored over 7 days. For this, the sensor was located in an acrylic chamber with a fixed volume (inner volume: 30 cm × 30 cm × 15 cm) for 30 min. When the sensor resistance was constant in ambient atmosphere (relative humidity: 50 − 60 %, room temperature), the banana was injected into the chamber and the variation of sensor resistance were measured for 300 sec, subsequently recovered to its original resistance via ejecting the banana from the chamber (operating temperature: 325 °C). The concentration of ethylene in the chamber were concurrently measured by PTR-QMS.

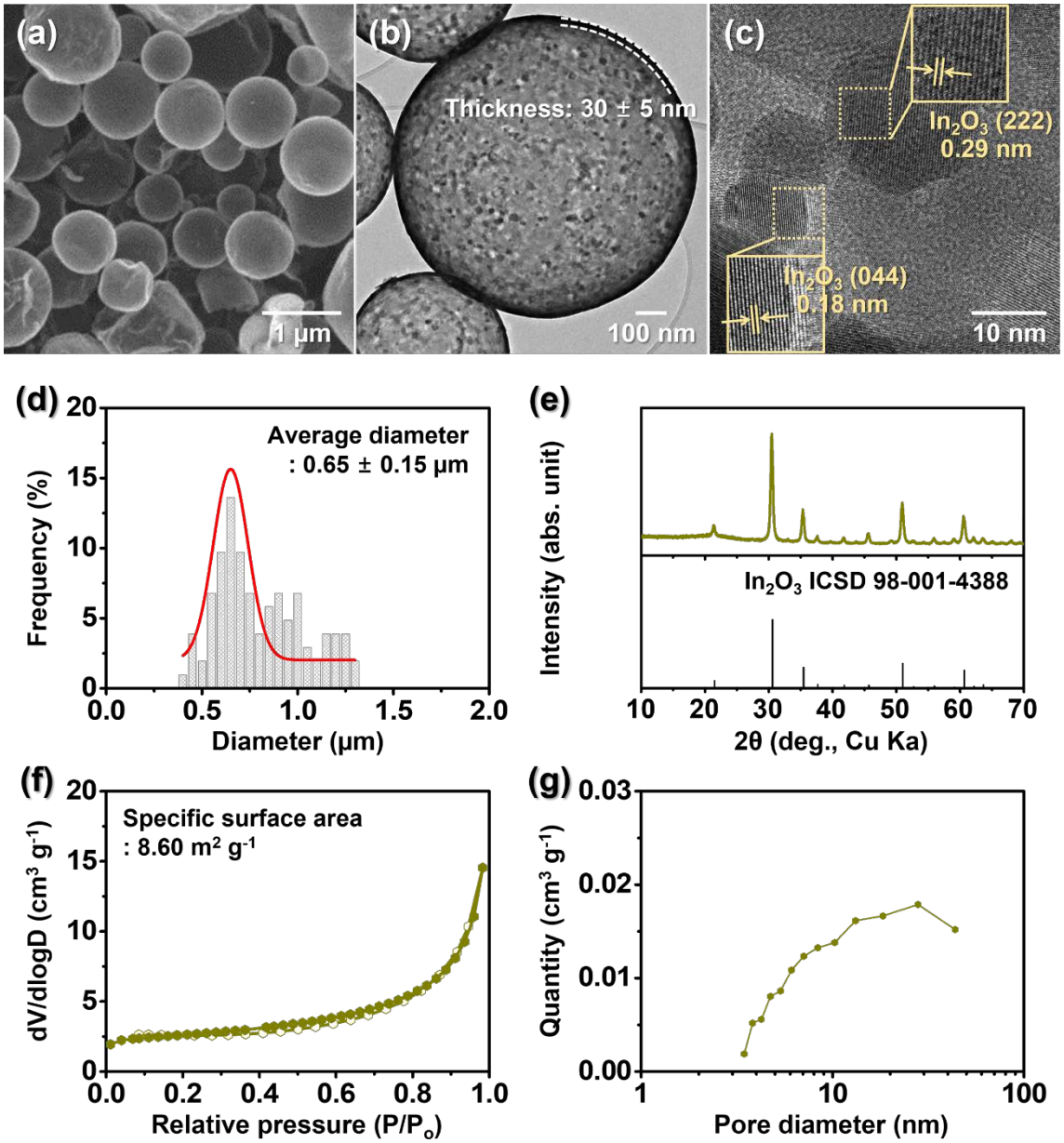

Fig. S1 (a) SEM image and (b) TEM image, (c) HR-TEM image, (d) size distribution, (e) XRD pattern, (f) N_2 adsorption/desorption isotherm and BET surface area, and (g) BJH pore-size distribution of In_2O_3 hollow spheres.

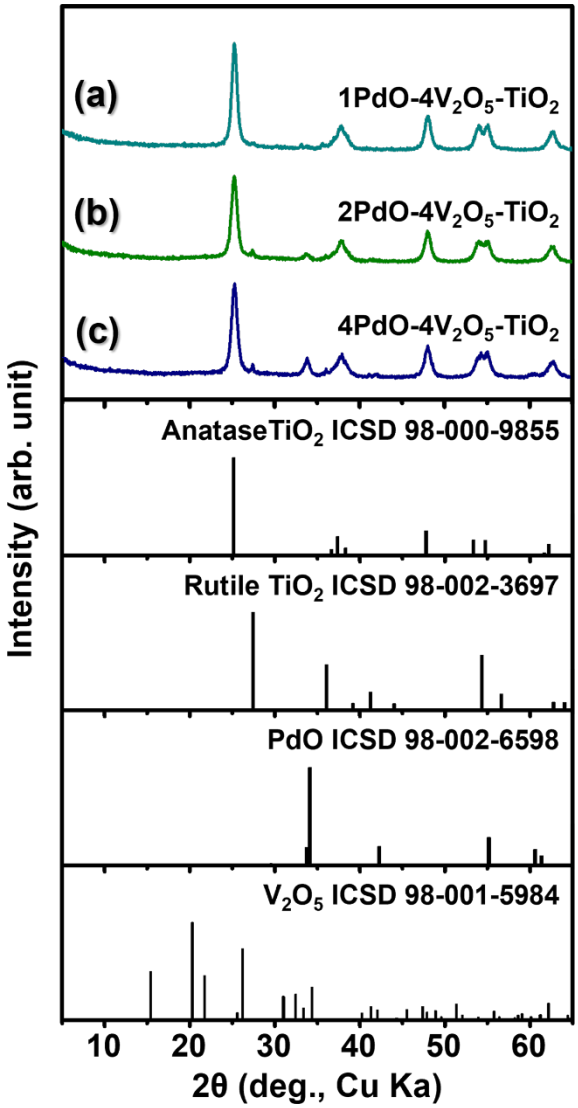

Fig. S2 XRD pattern of (a) 1Pd–V_2O_5–TiO_2, (b) 2Pd–V_2O_5–TiO_2, and (c) 4Pd–V_2O_5–TiO_2 yolk-shell spheres.

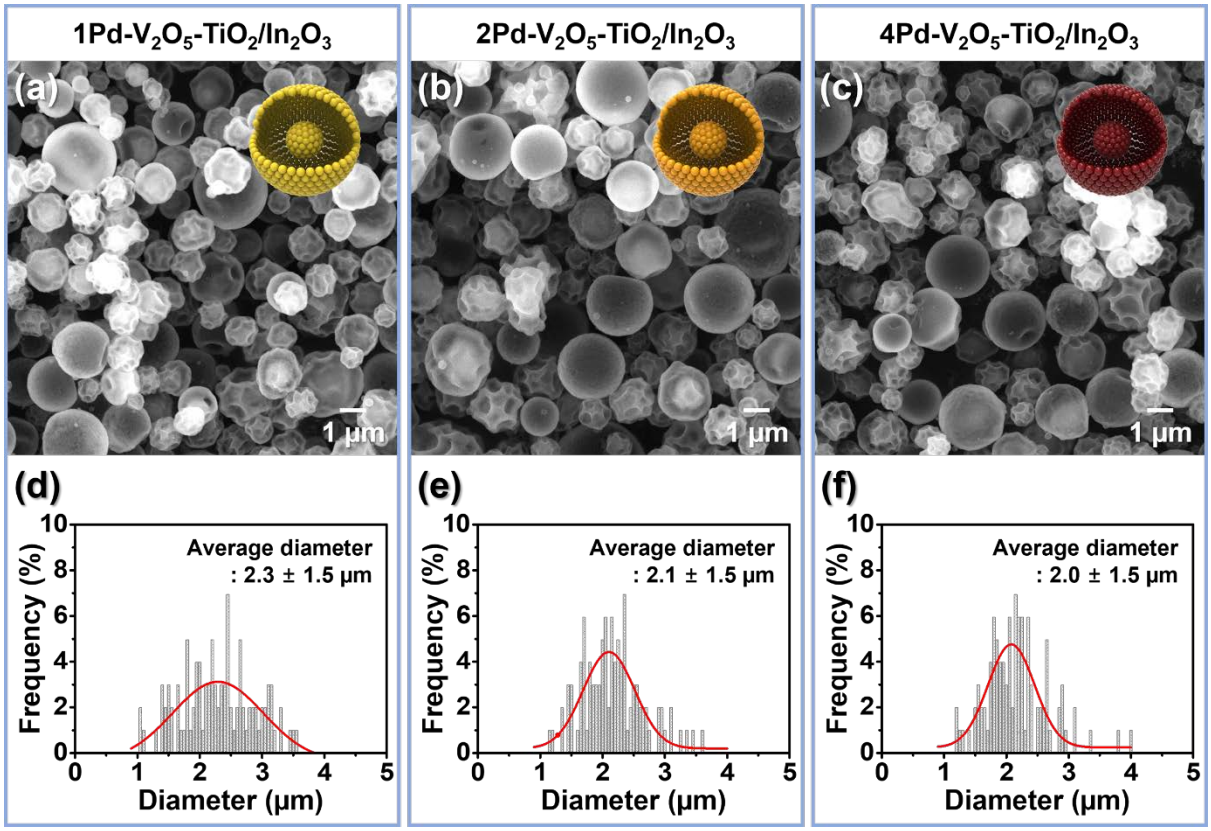

Fig. S3 (a-c) SEM images and (d-f) size distributions of (a and d) 1Pd–V_2O_5–TiO_2, (b and e) 2Pd–V_2O_5–TiO_2, and (c and f) 4Pd–V_2O_5–TiO_2 yolk-shell spheres.

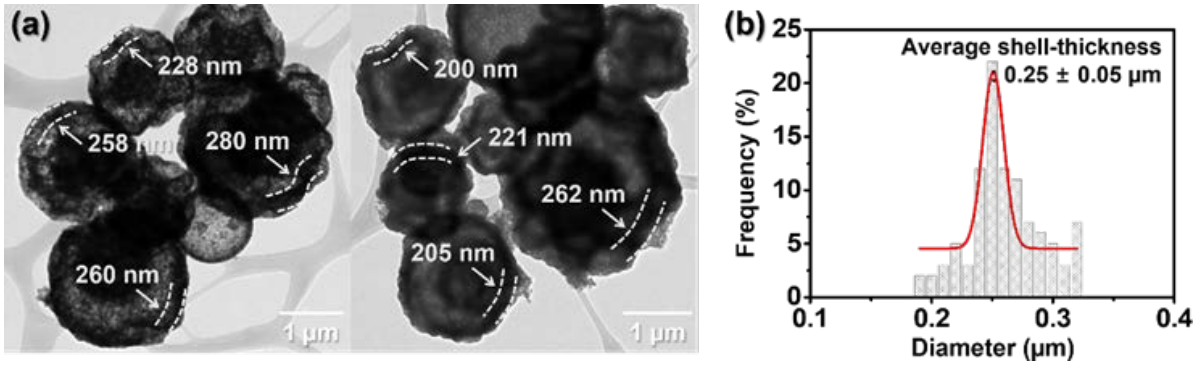

Fig. S4 (a) TEM images and (b) shell-thickness distribution of 2Pd–V_2O_5–TiO_2 yolk-shell spheres.

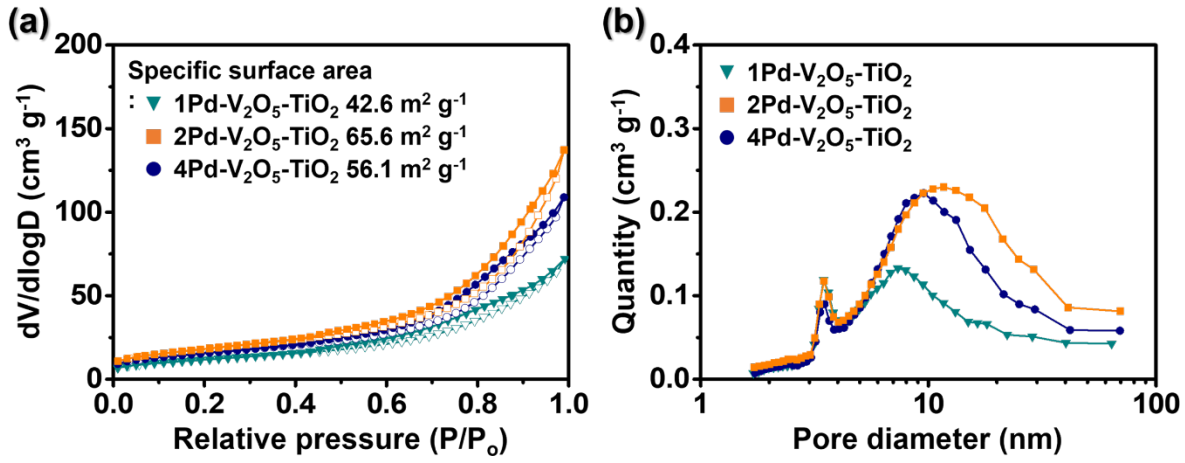

Fig. S5 (a) N_2 adsorption/desorption isotherms and BET surface areas and (b) BJH pore-size distributions of 1Pd–V_2O_5–TiO_2, 2Pd–V_2O_5–TiO_2, and 4Pd–V_2O_5–TiO_2 yolk-shell spheres.

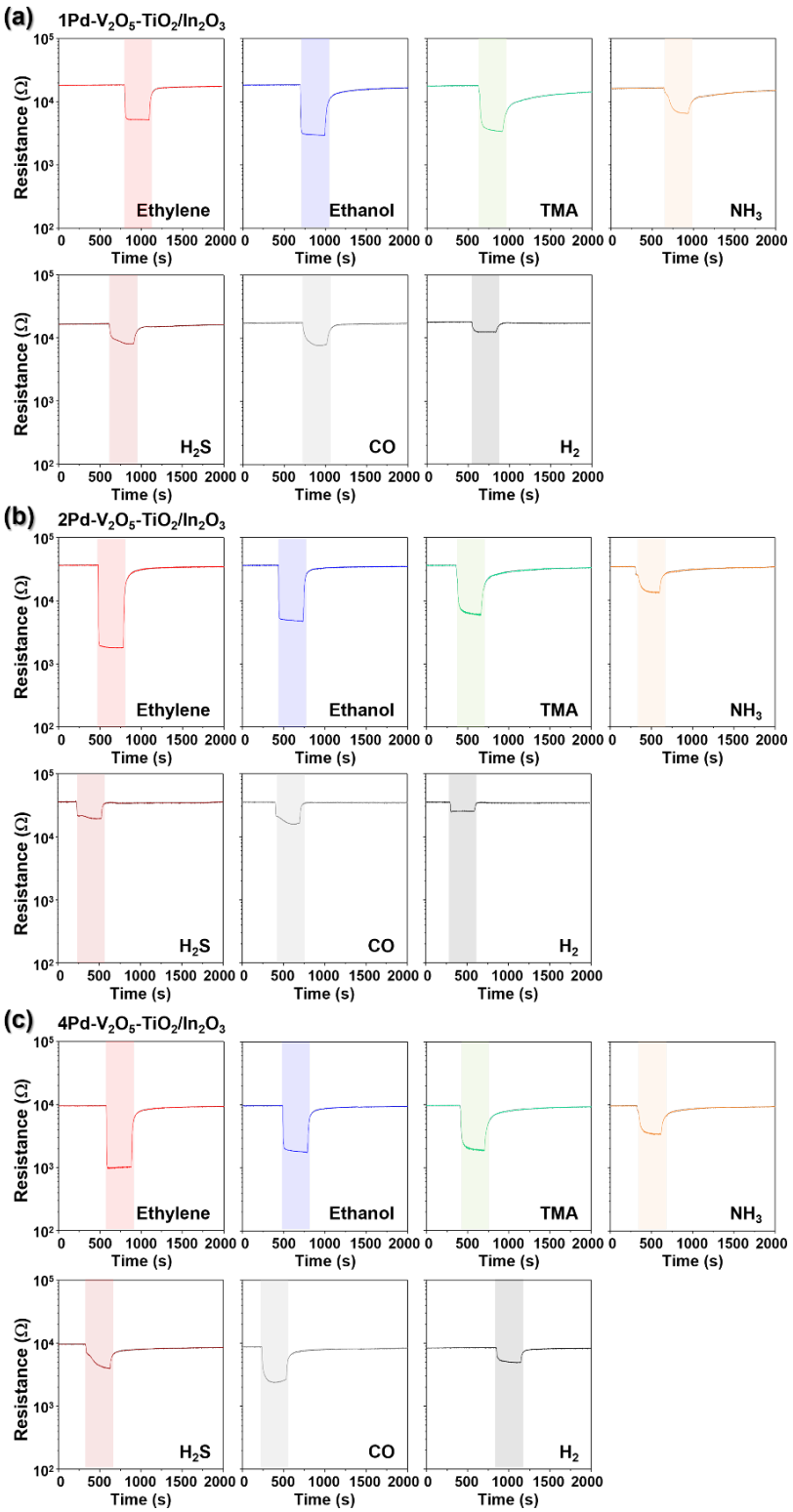

Fig. S6 Dynamic sensing transients of (a) 1Pd–V_2O_5–TiO_2/In_2O_3, (b) 2Pd–V_2O_5–TiO_2/In_2O_3, and (c) 4Pd–V_2O_5–TiO_2/In_2O_3 bilayer sensors to 1 ppm analyte gases at 300 °C.

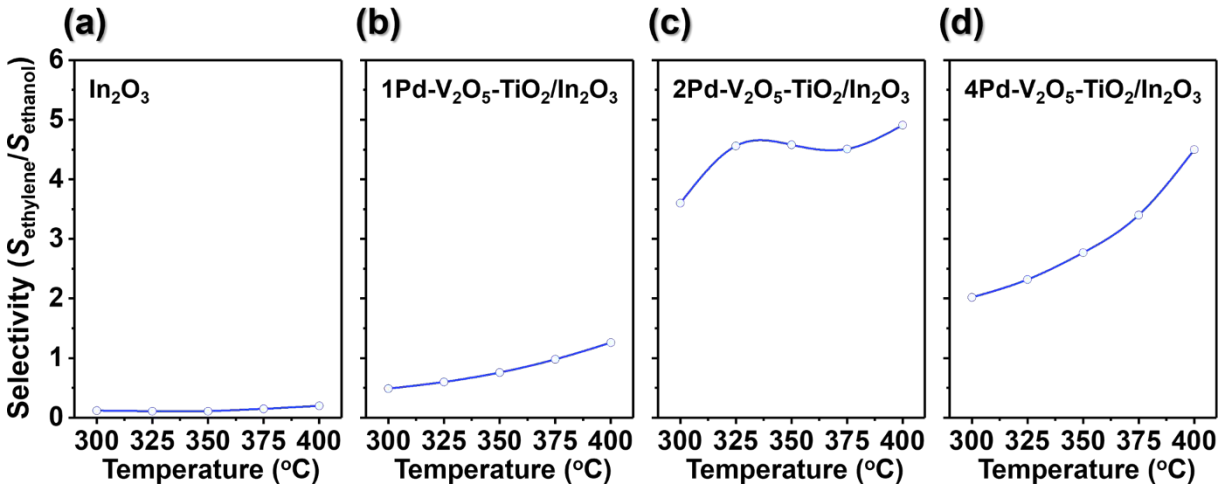

Fig. S7 Ethylene selectivity of (a) In_2O_3, (b) 1Pd–V_2O_5–TiO_2/In_2O_3, (c) 2Pd–V_2O_5–TiO_2/In_2O_3, and (d) 4Pd–V_2O_5–TiO_2/In_2O_3 bilayer sensors in the range of 300–400 °C.

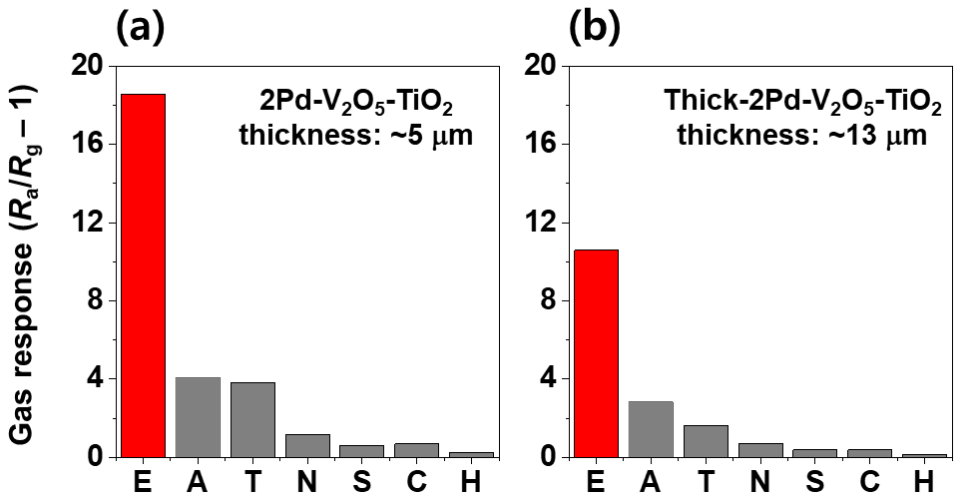

Fig. S8 Gas sensing characteristics of a) 2Pd–V_2O_5–TiO_2/In_2O_3 and b) thick-2Pd–V_2O_5–TiO_2/In_2O_3 sensors to ethyelne (E), ethanol (A), trimethylamine (T), ammonia (N), hydrogen sulfide (S), carbon monoxide (C), and hydrogen (H) at 325 °C.

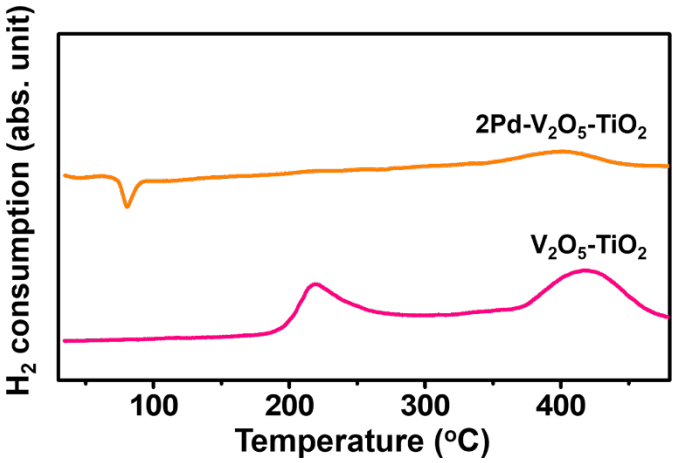

Fig. S9 H_2-TPR profiles of 2Pd–V_2O_5–TiO_2 and V_2O_5–TiO_2 catalysts under gradually increasing thermal conditions from room-temperature to 500 °C.

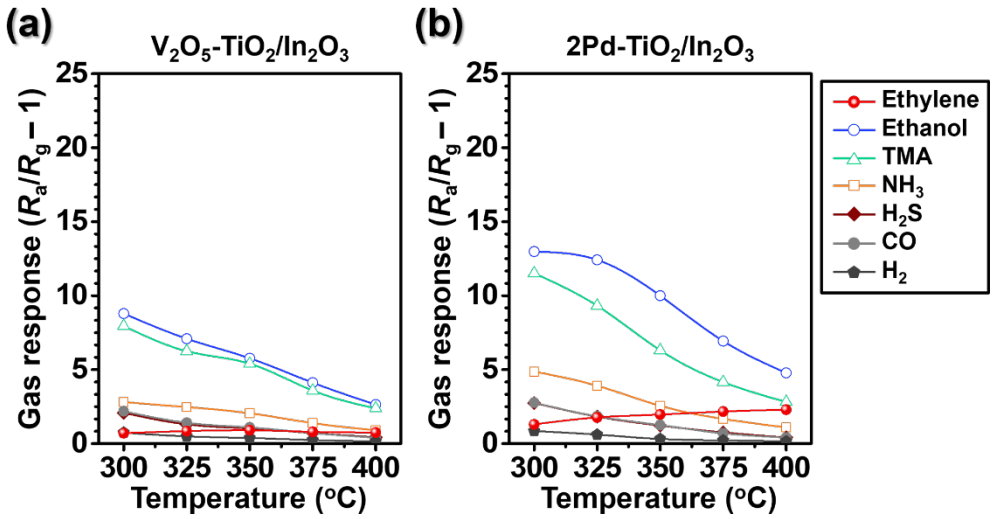

Fig. S10 Gas sensing characteristics of (a) V_2O_5–TiO_2/In_2O_3 and (b) 2Pd–TiO_2/In_2O_3 bilayer sensors to 1 ppm of various gases (ethylene, ethanol, TMA, NH_3, H_2S, CO, and H_2) in the range of 300–400 °C.

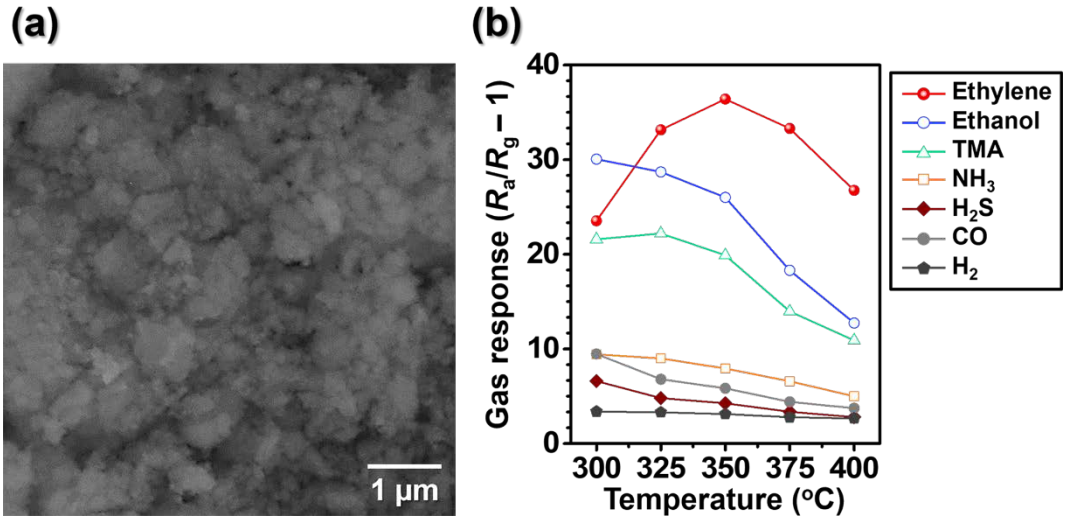

Fig. S11 (a) SEM image of NP-2Pd–V_2O_5–TiO_2 and (b) gas sensing characteristics of NP-2Pd–V_2O_5–TiO_2/In_2O_3 bilayer sensor to 1 ppm of various gases (ethylene, ethanol, TMA, NH_3, H_2S, CO, and H_2) in the range of 300–400 °C.

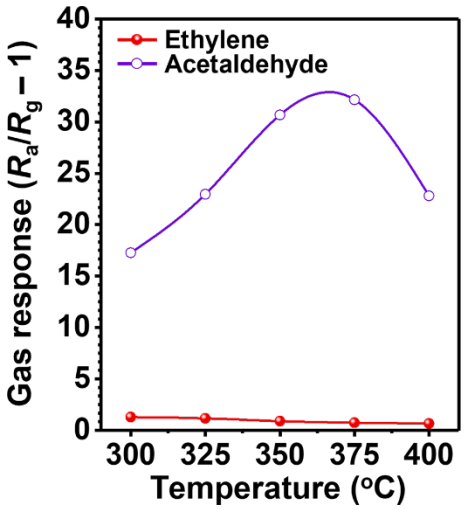

Fig. S12 Gas sensing characteristics of pure In_2O_3 sensor to 1 ppm of ethylene and acetaldehyde from 300−400 °C.

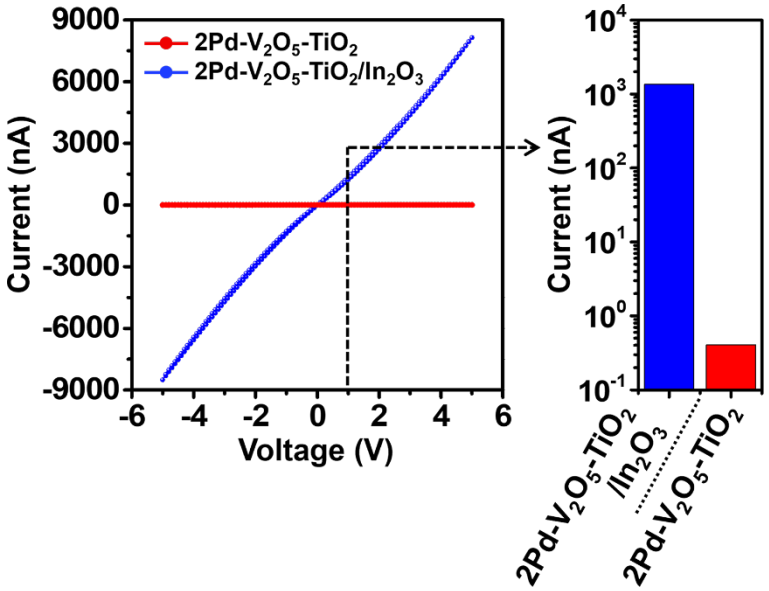

Fig. S13 I-V curve (left) and the current at 1V (right) of 2Pd-V_2O_5-TiO_2 single-layer sensor and 2Pd-V_2O_5-TiO_2/In_2O_3 bilayer sensor at 325 °C in air atmosphere.

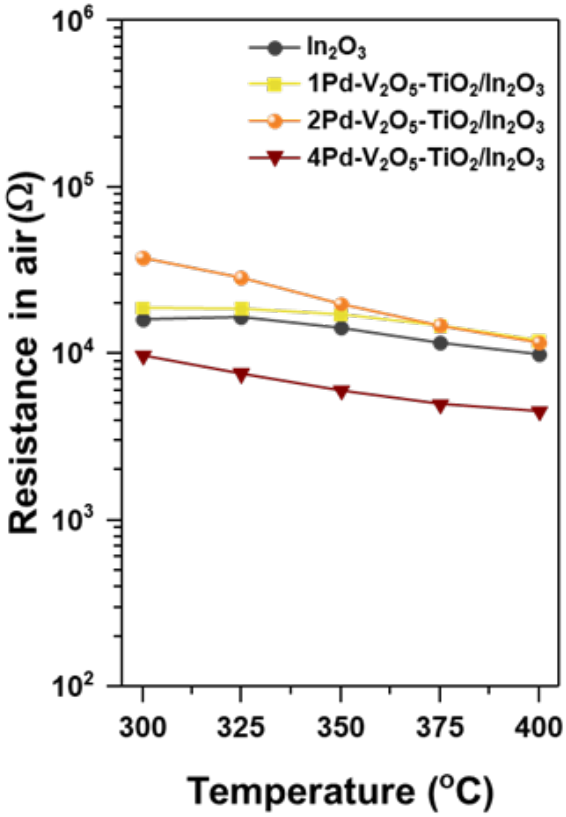

Fig. S14 Resistance in air of the In_2O_3 and xPd–V_2O_5–TiO_2 /In_2O_3 (x = 1,2, and 4 wt%) bilayer sensors in the range of 300–400 °C.